Available online at www.sciencedirect.com

SCIENCE DIRECT®

Thin Solid Films 467 (2004) 76–87

thin solid films

www.elsevier.com/locate/tsf

Bonding characteristics of DC magnetron sputtered B–C–N thin films investigated by Fourier-transformed infrared spectroscopy and X-ray photoelectron spectroscopy

V. Linss[a,*], S.E. Rodil[b], P. Reinke[c], M.G. Garnier[d], P. Oelhafen[d], U. Kreissig[e], F. Richter[a]

[a] TU Chemnitz, Institut für Physik, Physik fester Koerper, 09107 Chemnitz, Germany
[b] Instituto de Investigaciones en Materiales, UNAM, Circuito Exterior s/n, CU, Coyoacan, México D. F., Mexico
[c] Department of Materials Science and Engineering, University of Virginia, 116 Engineers Way, P.O. Box 400745, Charlottesville, VA 22904-4145, USA
[d] Departement für Physik und Astronomie, Klingelbergstr. 82, CH-4056 Basel, Switzerland
[e] Forschungzentrum Rossendorf, Postfach 510119, 01314 Dresden, Germany

Received 15 July 2003; received in revised form 9 January 2004; accepted 2 March 2004
Available online 21 April 2004

Abstract

B–C–N thin films of a wide composition range were deposited by reactive DC magnetron sputtering of targets with different B/C ratios in an Ar/N_2 atmosphere. The bonding characteristics of these amorphous films were investigated by Fourier-transformed infrared spectroscopy (FTIR) and X-ray photoelectron spectroscopy (XPS). The results of both characterisation methods indicate that real ternary compounds in which all three elements are bonded to each other are only formed when at least one element has a low concentration in the film—and therefore could be considered as an impurity. Otherwise the deposited material tends to a phase separation into binary compounds and single phases.

Keywords: BCN; Bonding characteristics; Fourier-transformed infrared spectroscopy (FTIR); X-ray photoelectron spectroscopy (XPS)

1. Introduction

In the last years, an increasing interest in materials of the ternary system B–C–N is observed. These materials are promising candidates for new compounds with adjustable electrical or mechanical properties because this system contains materials with extremely different properties that could be combined (superhard diamond and soft h-BN, semimetallic graphite and insulating h-BN). Several techniques have been used in order to deposit materials of the ternary system such as magnetron sputtering [1], pulsed laser deposition [2], chemical vapour deposition [3], shock wave compression [4] or high pressure/high temperature techniques (HP/HT) [5]. However, the attempts to deposit a real ternary compound failed in many cases. For example, magnetron sputtering under ion bombardment [6] as well as HP/HT [5] resulted in the deposition of diamond and c-BN but not in the combined cubic phase BC_2N (heterodiamond). In Ref. [7], we have given a more detailed summary of the aims of recent work in this field and the difficulties in depositing real ternary materials where all elements are bonded to each other. In that article, we also reported on first results on our reactive DC magnetron sputtered thin films in the B–C–N system. In this article, we want to give new results on the bonding characteristics of these films which were investigated by Fourier-transformed infrared spectroscopy (FTIR) and X-ray photoelectron spectroscopy (XPS). In contrast to Ref. [7], we will focus here on films deposited at floating potential because they show a completely amorphous structure [8]. The bonding characteristics are closely connected to the mechanical properties of the films. This and other structural properties of these films will be reported elsewhere [8].

2. Film deposition and characterisation

The films were deposited by reactive DC magnetron sputtering of targets with different B/C ratio (B, B4C, BC,

* Corresponding author. Tel.: +49-175-6130870; fax: +49-371-531-3042.
E-mail address: linss@physik.tu-chemnitz.de (V. Linss).

0040-6090/$ - see front matter © 2004 Elsevier B.V. All rights reserved.
doi:10.1016/j.tsf.2004.03.009

BC4, C) in an Ar/N_2 atmosphere on single-crystal silicon wafers (both sides polished for FTIR). The total pressure was 0.46 Pa and the N_2 content in the working gas was 0, 2%, 4%, 8%, 13%, 25%, 50%, 75% or 100%. The deposition was carried out at floating potential with a discharge current of 0.5 A without intentional substrate heating. More detailed information about the deposition process can be found elsewhere [7]. The bulk composition was measured by elastic recoil detection analysis (ERDA). In order to get information about the bonding characteristics transmission FTIR spectra in the range from 500 to 4000 cm^{-1} were recorded (Bruker IFS 66). Additionally, many films were investigated by XPS (VG ESCA-LAB210) in order to get complementary information. For the XPS measurements, monochromatised Al$K\alpha$ radiation was used. Several times, the Au $4f_{7/2}$ peak was measured for calibration and was found at (83.65±0.04) eV binding energy. First, a survey scan of every sample was made (50-eV pass energy, 0.5-eV step size) and then the B1s (if present), C1s, N1s and O1s peaks were measured in detail (20-eV pass energy, 0.05-eV step size). The XPS is a very surface sensitive method. Since the samples were measured ex situ contributions due to surface contamination (mainly O and C) were expected. In order to prove if this contamination can be desorbed, one sample was heated (200 °C) and one sputter cleaned (Ar^+). The heating removed only a small amount of O and C. The sputter cleaning changed the peak shape of the 1s spectra of all elements (much broader and/or shifted) because the original chemical bonding was changed. This effect is reported in the literature [9,10] but often neglected when XPS spectra are interpreted. Since pre-treatment introduces undesirable changes to the film all measurements reported in this article were carried out without cleaning the surface and the contributions of the contamination have to be taken into account. The XPS spectra of a few samples showed a shift in binding energy of the elemental peaks due to electrical charge during the measurement which has to be corrected before comparing the spectra. Only if all elemental peaks show the same shift a homogenous charge of the sample can be assumed and corrected. This was the case for all charged samples. Peakfitting (of the XPS spectra) with Gaussians was carried out but will not be considered here because due to the surface contamination quantitative statements are difficult to make. We will concentrate on qualitative dependences.

3. Composition

The bulk composition of the samples has already been given in Ref. [7]. As impurities, O and H were detected (mostly below 5 at.% for each element). Fig. 1 compares bulk composition (ERDA) and surface composition (XPS) of samples deposited from the B4C and BC4 targets. The composition according to B–C–N (that means without impurities) is represented by the position in the ternary triangle while the oxygen content according to B–C–N–O–H for the ERDA and B–C–N–O for the XPS (H cannot be detected with XPS) is indicated by the height over the triangle. Obviously, the surface contains more O (6–15 at.%) than the bulk and the composition is shifted towards C while the B/N ratio stays nearly the same (see lines of constant B/N ratio in Fig. 1). The deviation of the surface composition from the bulk composition can be due to the deposition process (uncontrolled particle flux after closing the shutter). However, more likely is an adsorption of mainly hydrocarbons and water after the removal of the samples from the vacuum equipment. A few samples were measured by ERDA again after the XPS measurements. For this measurement, a higher sensitivity near the surface was achieved by a smaller incidence angle of the Cl^{7+} ions. However, the former ERDA results were reproduced. It can be supposed that the surface contamination was only more or less a monolayer which was rapidly removed by the ion beam used for the ERDA measurement. Since a surface contamination with a B containing substance is unlikely the B1s spectra should be the most precise for the interpretation of the bonding characteristics.

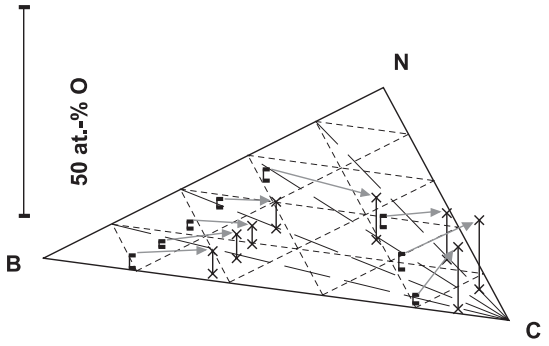

Fig. 1. Comparison of the compositions relating to B, C and N of bulk (determined by ERDA, represented by bars) and surface (determined by XPS, represented by crosses) of samples deposited with the B4C and BC4 target. The oxygen content is represented by the height over each point (see 50 at % scale on the left hand side).

In the following, the bulk composition of the samples will be given in the figures for each experimental series.

4. Bonding characteristics

Before looking at spectra, some comments on their interpretation should be made. XPS and FTIR are widely used for the identification of chemical bondings. However, it is often neglected that conclusions might be difficult to draw. If a certain chemical environment is expected, the respective peaks should be contained in the spectra. The reverse way is not clear. An observed peak does not necessarily identify a certain chemical bond because different chemical surroundings may lead to the same peak shift.

However, in many cases, the difference in peak shift is sufficient to *exclude* a certain type of bonding. In addition, the interpretation of the core level spectra of one element should be consistent with that of all other elements in the sample. The interpretation that broad peaks indicate real ternary bonding (see, for example, Ref. [11]) may be wrong because the atoms of one element could be distributed inhomogeneously and the observed bonding energies are due to the distribution in different chemical surroundings. In principle, it is not possible to distinguish a certain bond because the binding energy of the 1s core level is influenced by the complete chemical environment of the atom. For example, the "B–C" bond cannot be identified clearly in the B1s spectrum because it depends on which other atoms are bonded to that B atom (N–B–C will have a different B1s binding energy as C–B–C). Actually, each chemical environment leads to a defined binding energy. If there is a uniform chemical environment, mainly one peak should occur in the 1s spectrum of the according element. In contrast to that, for example, Saugnac et al. [12] found several peaks in the B1s spectrum of their ternary samples and interpreted those peaks as bonds to C and N. They suggested a graphitic structure in which B is always bonded to two C atoms and one N atom in the graphitic plane. However, that would mean equal chemical environment for each B atom and therefore only one main peak should have been present in the B1s spectrum. Another difficulty in peak assignment arises from the relaxation contribution to the binding energy which differs in molecules and solids and thus makes a direct comparison of XPS spectra of molecules and solids complicated [10].

The picture is much clearer in the case of the FTIR spectra. Here, the peak position is determined by the bond strength and the mass of the two bonded atoms. Shifts in the order of a few 10 cm^{-1} occur due to the chemical environment of each atom. By substitution of one atom in the bond by its isotope, the bond can clearly be identified [13,14] because the bond strength stays the same and the mass is changed. Some peak positions are widely accepted in the BCN literature. The B–N stretching bond is found at approx. 1380 cm^{-1}, the B–N–B bending at approx. 780 cm^{-1} and the C≡N bond at approx. 2200 cm^{-1}. Furthermore, the absorption due to H impurities (stretching) is commonly found at approx. 2500 cm^{-1} for B–H, approx. 2900 cm^{-1} for C–H and approx. 3300 cm^{-1} for N–H. The peak position at approx. 700 cm^{-1} is assigned to a bending bond of graphitic C [15] but is also found in B_4C [16]. Other peak positions are discussed with much more controversy. Especially the absorption positions of B–C and C–N bonds are not very clear. Sometimes, the composition of the films seems to play a role. The B–C bond for example is found between 1070 and 1250 cm^{-1} where B-rich films have a maximum absorption at 1100 cm^{-1} and C-rich ones at 1250 cm^{-1} [17]. Probably, a different structure leads to different bondings and hence absorption. Even more confusing is the discussion about a broad absorption structure found especially in CN_x but also in BCN films between 1000 and 1700 cm^{-1}. Several bonds should contribute to this absorption. Often, the position around 1300 cm^{-1} is assigned to C–N bonds (for example, Refs. [18–20]) and around 1600 cm^{-1} to C=N bonds (for example, Refs. [21,22]). However, there was no isotopic shift when ^{14}N was replaced be ^{15}N [13,14] indicating that N is not a partner in this bond. Also, absorption in this range is found in a-C/H films without N [23]. Obviously, the bonds absorbing in this range are C–C bonds of different types. An interpretation can be found in Refs. [13,23].

4.1. Films deposited without N_2 in the working gas

In this section, we consider samples deposited without N_2 in the working gas. The N-incorporation due to the background pressure and target poisoning was about ≤2 at.% in the bulk (ERDA result) and <4 at.% at the surface (XPS result) except for the sample deposited from the BC target which had more than 11 at.% N on the surface (and also more than 18 at.% O). The FTIR as well as the B1s and C1s XPS spectra of these samples are shown in Fig. 2. Since the samples had similar film thickness, the FTIR absorption can be directly compared. The XPS spectra are scaled to the same maximum height (see scaling factor over each spectrum). For the samples deposited from the pure B and C targets, only the interference pattern due to the film thickness can be seen. There is only a weak absorption in the spectra of the sample from the B target at 1050 cm^{-1}, probably due to the incorporation of O and C from the deposition process, resulting in a polarisation of the B–B bonds. When C is added to B (sample from the B4C target), an absorption around 1100 cm^{-1} appears. Two contributions are expected: polarised B–B bonds and polar B–C bonds. When B is added to pure C (sample from the BC4 target), an absorption is found at 1300 cm^{-1}. Here, polarised C–C bonds and B–C bonds are expected. Literature reports 1264 cm^{-1} [24], 1300–1400 cm^{-1} [23] or 1400 cm^{-1} [25] for the C–C stretching bond. The different contributions of polarised B–B, B–C and polarised C–C bonds may explain the absorption shift for B-rich and C-rich B–C bonds mentioned in the literature [17]. The FTIR spectrum of the sample with equal concentrations of B and C (from the BC target) looks like a superposition of the spectra of the samples deposited from the B4C and BC4 target. However, there is no information if this is a homogenous elemental mixture or two phases put together causing the absorption structure.

The XPS spectra give further information about the bonding structure. First, we consider the B1s spectra. The B1s spectra from the samples deposited from the B and B4C target show a single broad peak at similar binding energy, indicating similar chemical environments. With C in the film, the maximum of the peak shifts slightly to a higher binding energy (187.6 to 188 eV) because the incorporated C is more electronegative. The peak positions are consistent

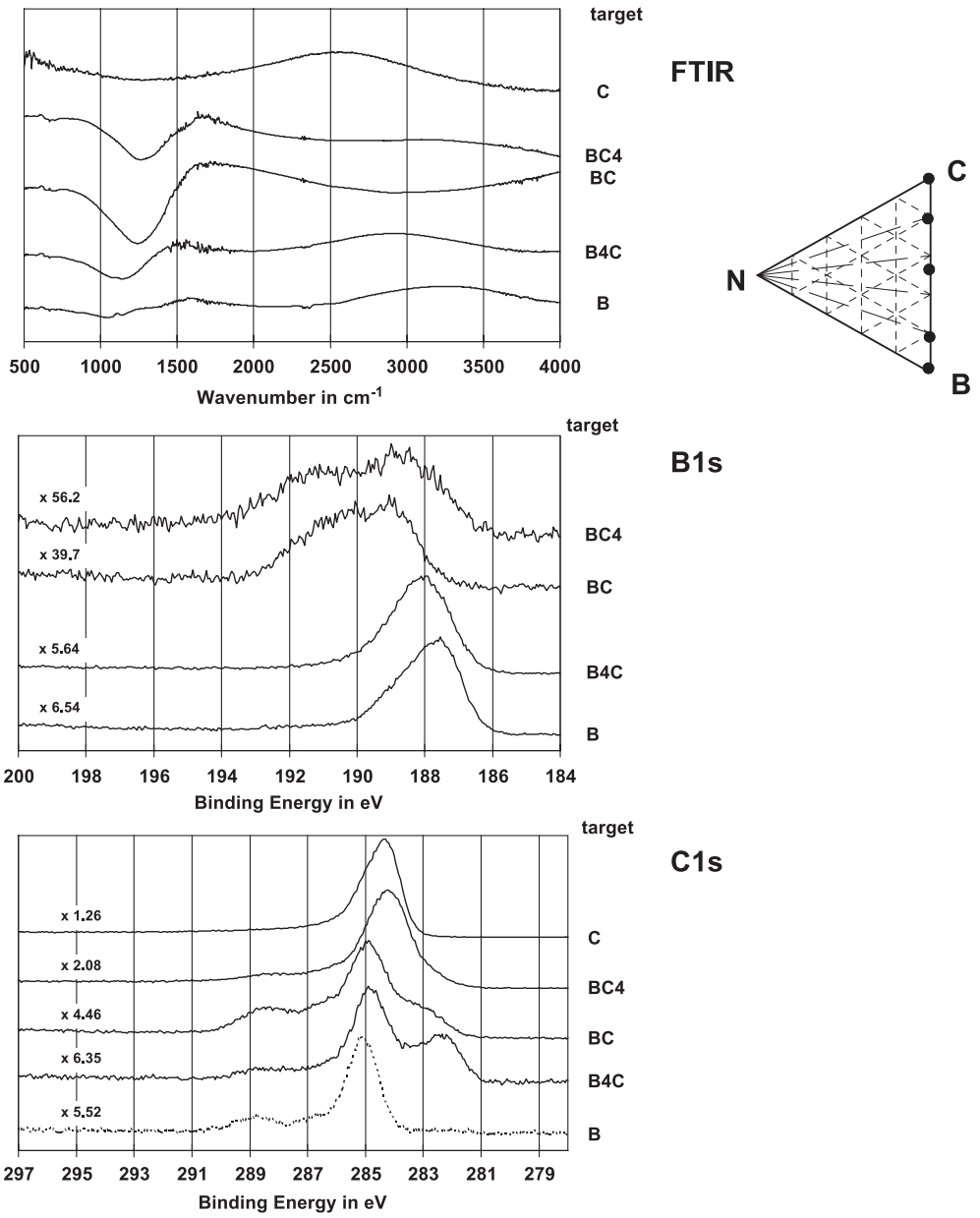

Fig. 2. Transmission FTIR, B1s and C1s XPS spectra (stacked) together with the bulk composition of samples deposited without N_2 in the gas. The dashed C1s XPS spectrum is due to the surface contamination during the ex situ measurement.

with some references in the literature (B in Refs. [26–28], B_4C in Refs. [17,29,30], however, other groups give different values). When more C is added to the film, two peaks can clearly be distinguished in the B1s spectrum (samples from the BC and BC4 target). Since the surface of the sample from the BC target was heavily contaminated, we will focus on the sample deposited from the BC4 target. The two peak maxima are found at 188.8 and 191.0 eV. The first fits well in the trend of the peak shift to higher binding energy of the B1s when more C is incorporated into boron. The second, with higher binding energy, gives evidence that B atoms themselves are embedded into a more electronegative environment. The existence of stoichiometric boron oxide can be excluded because the binding energy would by even higher than 193 eV [28,31]. Hence, since there is almost no N in the film, the only possible explanation is that B is incorporated between C atoms. Thus, the B1s spectra give indication that we have two chemical states of the B atoms, namely boron in which C atoms are embedded up to a certain content and B atoms which themselves are embedded into a carbon environment. Can the C1s spectra confirm this interpretation? The contribution of the significant carbon surface contamination has to be considered and can be seen from the C1s spectrum of the film deposited from the B target (dashed spectrum in Fig. 2). Here, only C from the surface contributes to the spectrum. In contrast to

that, in the case of the film deposited from the C target, the relative contribution of the surface contamination is very much weaker. This spectrum shows one peak with the maximum at 284.4 eV which is typical for graphitic or amorphous carbon. The incorporation of 20 at.% B (sample from the BC4 target) leads to a broadening of the peak towards lower binding energies which can be explained by the lower electronegativity of the B atom. The binding energy is lower, the more carbon neighbours of a C atom are exchanged by B atoms. This effect is stronger in the C1s spectrum of the sample from the BC target. However, the surface of this sample was heavily contaminated and so also structures at higher binding energies contribute to the spectrum (bonds between C and N, O). Finally, the spectrum of the sample from the B4C target gives evidence that C in the bulk is mainly surrounded by B atoms. Here, the contributions of the surface contamination (compare dashed spectrum) and a peak with the maximum at 282.5 eV can be distinguished which is commensurate with the binding energy of about 283 eV found for B_4C [11,17,28].

From all spectra together, we can conclude that starting from pure boron a certain amount of C atoms can be incorporated (up to about 20 at.%). With further increasing C content two phases are formed: a boron phase with a maximum content of incorporated C atoms and a carbon phase which contains B atoms as impurity. This interpretation is supported by the number of nearest neighbours as measured by electron diffraction. It is approx. 5 and 4.5 for the samples from the B and B4C targets, respectively, but only 2.5 for the film from the BC4 target [8]. Also for the crystalline phase, the incorporation of carbon into boron is limited in the range $B_{12}C$ to $B_{4.3}C$ [32].

4.2. Films deposited with 50% N_2 in the working gas

Now, we want to consider the samples deposited with 50% N_2 in the gas from the different targets. The N content in the film is close to the maximum content reached by deposition with 100% N_2 in the gas. The FTIR and XPS spectra are shown in Fig. 3. In the case of the film from the B target, only the FTIR spectrum was recorded. The peak intensities in the FTIR spectra can be compared because the films had similar thickness, only the sample from the C target had approx. twice the thickness. The FTIR spectra show an absorption between 600 and 800 cm^{-1} consisting of two contributions which change with the B/C ratio in the film. These are the B–N–B bending (around 780 cm^{-1}, very significant in the spectrum of the film from the B target) and probably a C–C bond (around 700 cm^{-1}). The broad absorption structure of the BCN films between 1000 and 1700 cm^{-1} consists of different contributions as well. In the case of the BN film without C, only the absorption of the B–N stretching bond around 1400 cm^{-1} exists. In the case of the CN_x film without B, at least two contributions can be distinguished. The appearance of these absorptions has been discussed at the beginning of Section 4 and their origin is in our opinion found in carbon bonds, but in the literature often assigned to C–N or C=N bonds. The spectra of the films from the B4C, BC and BC4 targets seem to be a superposition of the spectra from the BN and CN_x film. That B–N and C–C bonds are present has already been proven by the absorption around 700 cm^{-1}. The absorption of the C≡N bond around 2200 cm^{-1} gives evidence that N is also bonded to C. However, whether C–N or C=N bonds are also present cannot clearly be found out. Besides, it cannot be concluded if there are B–C bonds as well because they would undistinguishably contribute to the broad absorption structure. At approx. 3400 cm^{-1}, the absorption of the N–H stretching bond is found. This peak shifts slightly to lower wavenumbers with increasing C content and is missing in the spectrum of the film without boron although N and H are incorporated.

The XPS spectra should give further information about the bonding structure. The B1s spectra look very similar. There is only one peak at about 191 eV. Only in the spectrum of the sample from the B4C target the maximum is found at slightly higher binding energies and there is an asymmetry to lower binding energies. A B1s energy of 191 eV is found in BN or when B atoms are completely embedded in carbon (according to the interpretation developed in Section 4.1). The C1s spectra do not indicate a sizeable contribution from B–C bonds and thus favour the assignment of this peak to BN for most of the films. All C1s spectra are characterised by a maximum at approx. 285 eV and there is a sharp drop of the spectra to lower binding energies. Only the C1s spectrum of the film from the B4C target shows a little contribution also below 284 eV which indicates that some C atoms are at least partly bonded to a less electronegative partner (B atoms, confirmed by the small low energy tail of the respective B1s spectrum). The C1s spectrum of the sample from the BC target has its maximum at 285.3 eV. The maximum shifts slightly to lower binding energies when more C is in the film (films from BC4 and C target, respectively) which is due to an increasing number of carbon neighbours of a given C atom (284.4 eV). On the other hand, all spectra show a broad shoulder to higher binding energies. It is interesting to note that the extension of that shoulder (area) related to the maximum peak at about 285 eV shows the same dependence on the B/C ratio in the film as the absorption strength of the C≡N bond at 2200 cm^{-1} in the FTIR spectra (increase for the films from the B4C, BC and BC4 targets, then decrease for the film from the C target). C1s energies >285 eV are assigned to C atoms which are bonded to the more electronegative N. Here, the literature is very ambiguous as demonstrated in Ref. [33]. Many groups assign binding energies to certain bonds, for instance: sp^2 hybridised carbon with bondings to nitrogen (285.3 eV in Ref. [34], 285.5 eV in Refs. [35,36], 285.9 eV in Refs. [21,37,38], 286.3 eV in Ref. [39], 287.7 eV in Ref. [40]), sp^3 hybridised carbon with bonding to nitrogen (285.7 eV in Ref. [40], 286.8 eV in Ref. [35], 287.3 eV in Ref. [41],

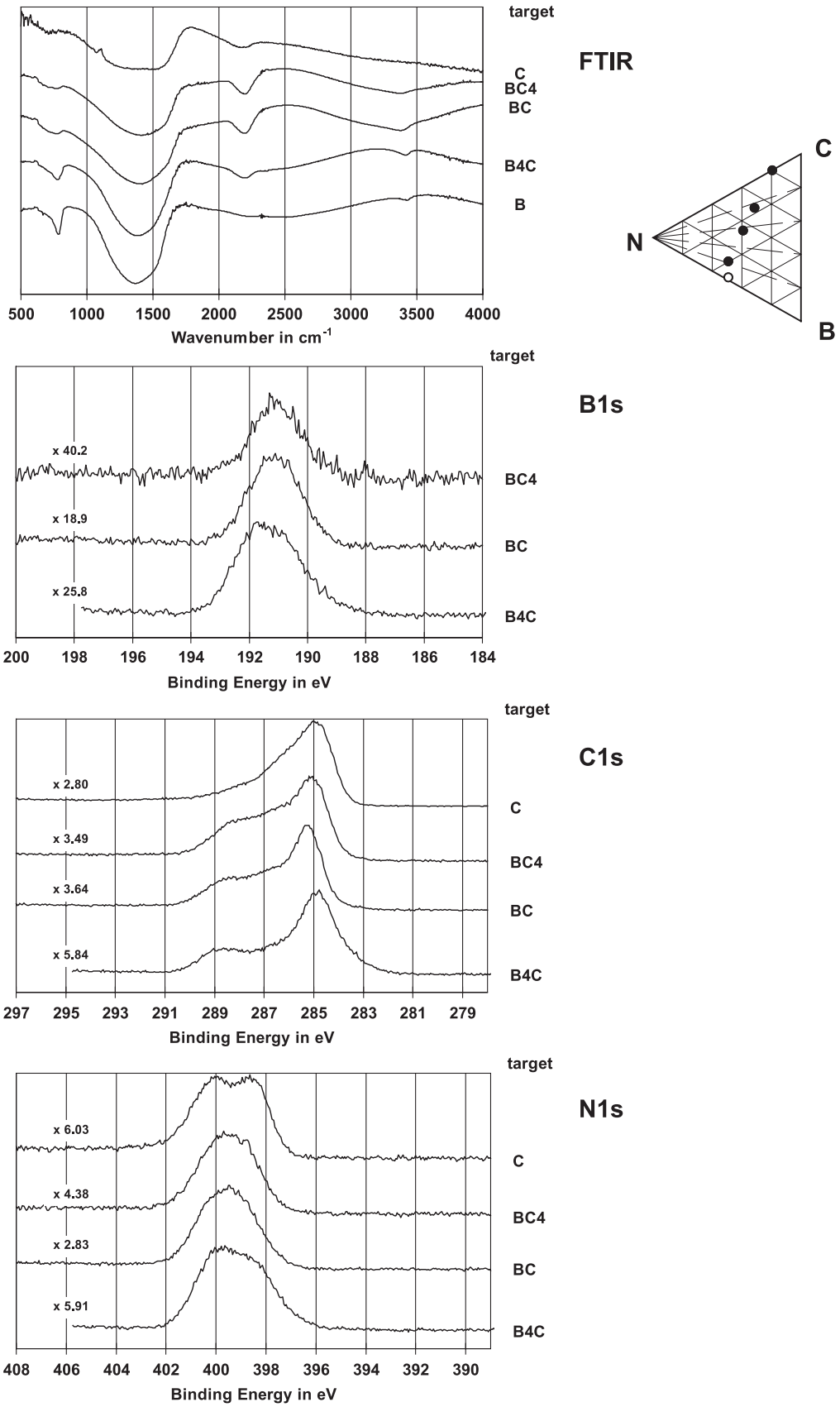

Fig. 3. Transmission FTIR, B1s, C1s and N1s XPS spectra (stacked) together with the bulk composition of samples deposited with 50% N_2 in the gas. For the sample marked by an empty circle in the composition graph, only the FTIR measurement was done.

287.7 eV in Refs. [39,42]) or the –C≡N bond (286.4 eV in Ref. [34], 286.7 eV in Ref. [38], 287.2–287.7 eV in Ref. [10]). However, an unequivocal assignment is missing (and cannot exist due to the large number of possible bonding states and atomic arrangements between C, N). Only the fact that C is anyhow bonded to N is clear. In our spectra, the wide observed binding energy range gives evidence for many bonding states between C and N (single, double or triple bond, different kind and number of neighbour atoms). The N1s spectra are not of great help to find out more about the bonding states because the energy range for N atoms with bondings to B and C is relatively small and the interpretation is again ambiguous [33]. We only can exclude bondings to O or N itself because no binding energies above 401 eV [42–44] are observed. The N1s spectrum of the sample deposited from the C target has at least two separate peaks at 398.5 and 400.0 eV which is often observed for CN_x films. Some references [35–37,39,42,45] assign these energies to N which is bonded to sp^3 and sp^2 hybridised carbon, respectively. However, in our spectrum, the peaks have nearly the same contribution but the average number of nearest neighbours in the film is only about 2.5 [8] which indicates that there is no significant number of sp^3 hybridised atoms. Other references [46–48] assign these energies to C≡N and C=N, respectively, what seems to be a better interpretation in our case. Ripalda et al. [49] found a strong polar emission angle dependence for the lower energy component in the N1s spectrum and conclude that it is associated to strong π bonding. The two peaks found in the N1s spectrum are assigned to N in low coordination number environments (double and triple bonds) and to substitutional nitrogen in graphitelike structure, respectively [50,51]. This assignment seems to be reasonable for our films as well. However, the only conclusion is that in our films, different bonding states between C and N exist, which exactly cannot be concluded. Probably, the localisation of the lonely electron pair of the nitrogen plays an important role. The situation gets even more confusing if B is added to the film. Then, the spectrum has its maximum at 399.5 eV (films from the BC4 and BC targets) which could be due to an additional third component compared to the spectrum of the film without B. However, the N1s binding energy observed in h-BN is 398.4 eV [31]. What could explain the higher binding energy of the N1s in our films? This could be due to another more electronegative bonding partner of N in addition to B which could be C or N. The spectrum of the sample from the B4C target shows again the two separate peaks but additionally, a tail to smaller binding energies. However, this sample had a strong surface contamination (see Fig. 1) and so a major part of the peak shape originates from the contaminating substance.

Summarising the results of all spectra, we can say that the number of B–N–B bonds in the films is decreasing with decreasing B/C ratio. Instead, the number of C–C chains is increasing. There are also bonds between C and N. The C≡N bond is evidenced by the FTIR spectra, the C1s spectra confirm many other bonding types. Only in B-richest film which was investigated with XPS (from the B4C target) B–C bonds were present (confirmed by the low energy contributions in the B1s and C1s), likely in connection with bonding to N. For the other B containing films (from the BC and BC4 target), we can assume that B is surrounded by N and so N is a separator between B and C. Therefore, a N1s energy higher than in h-BN is observed but the low energy contributions in the C1s and B1s are missing. Furthermore, there are bonds between C and N and between C and C. Hence, we find a phase separation on a microscopic scale into BN and C/CN_x phases in the sense that microscopic domains with mainly B–N bonds on the one hand and mainly C–C as well as C–N bonds on the other hand are present but bonds between B and C are avoided. Therefore, the FTIR spectra of BCN films look like a superposition of the spectra of BN and CN_x films. There is a real ternary bonding in the sense that N is bonded to B and C (B–N–C). However, B–C bonds are only found in the case of B rich films.

4.3. Films deposited from the B4C target

In the two previous sections, we have considered what changes can be observed when the B/C ratio in the film is varied. Now, we want to consider increasing N-incorporation at nearly constant B/C ratio and start at a ratio of B/C=4:1 (spectra in Fig. 4). The FTIR spectra of the films deposited from the B4C target show continuous changes with increasing N content. Without N in the film, there is only one absorption around 1100 cm^{-1} due to B–C and/or polarised B–B bonds, as mentioned in Section 4.1. Increasing the N content, the maximum of the peak shifts towards 1400 cm^{-1} where B–N stretching bonds vibrate. At the same time, the asymmetry to lower wavenumbers decreases and vanishes suggesting that the number of B–B and/or B–C bonds is decreasing. The film deposited at 4% N_2 in the gas (22 at.% N in the film) shows a slight absorption around 700 cm^{-1} which can be assigned to the (polarised) C–C stretching bond or an absorption observed in B_4C. This absorption is also present in all films containing more N than 20 at.%. The film deposited with 8% N_2 in the gas (34 at.% N in the film) shows the absorption of the B–N–B bending at 780 cm^{-1} which gets more dominant with increasing N content. Obviously, the formation of B–N–B chains is accompanied by the decrease of B–B and/or B–C bonds and the material shows significant structural changes. With increasing N content, the average number of nearest neighbours decreases and the low-energy EELS spectra of films deposited with ≥8% N_2 in the gas show a plasmon-peak at 7–8 eV which is typical for sp^2 hybridised C or BN (graphitic structure) [8]. Furthermore, in the films deposited with 25% up to 100% N_2 in the gas, the absorption of the C≡N bond at 2200 cm^{-1} appears and gets stronger although the N content in the film is not changed significantly. In particular, especially the films

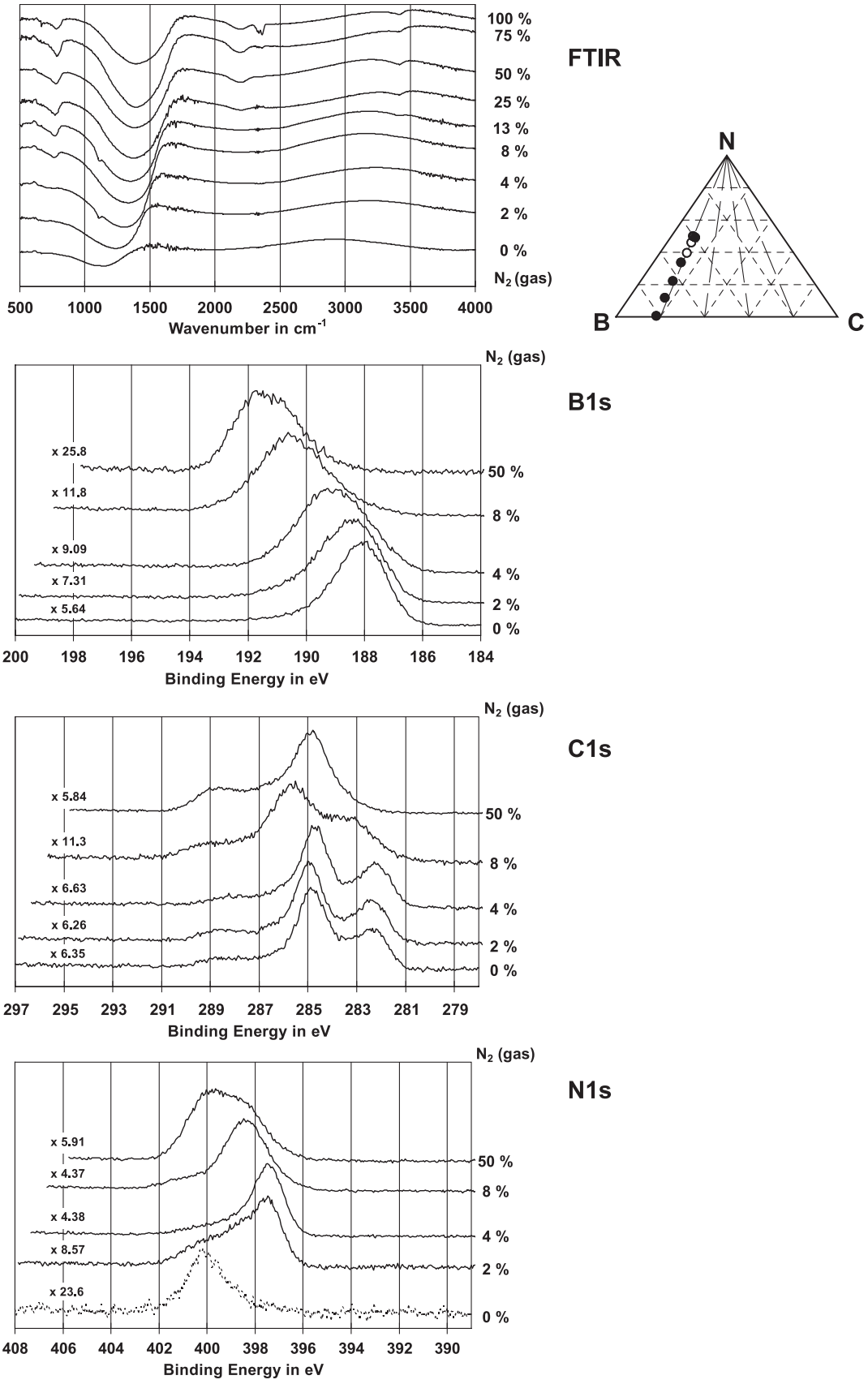

Fig. 4. Transmission FTIR, B1s, C1s and N1s XPS spectra (stacked) together with the bulk composition of samples deposited from the B4C target. For samples marked by empty circles in the composition graph, only FTIR measurements were done. Samples deposited with 50%, 75%, 100% N_2 have nearly identical composition [7].

deposited with 50%, 75% and 100% have nearly identical N contents [7]. This means that at a certain N content in the film, the B–N bonds are saturated and additional N is incorporated in terminating C≡N bonds. The N–H bond at 3400 cm^{-1} can be detected from 13% N_2 in the gas and gets stronger with increasing N content. It is interesting to note that the position of this absorption peak does not change like in the case of changing B/C ratio (Fig. 3).

The XPS spectra confirm these changes in structure and bonding characteristics. With increasing N content, the B1s peak gets broader and the spectrum is shifted to higher binding energies. First, the incorporated N is embedded into the B/C=4:1 mixture and the B atoms are surrounded by more and more N until most of them are completely embedded into N. Then, the B1s binding energy is higher than observed in BN (approx. 191 eV [26,31,52]). All the C1s spectra of the films deposited with <8% N_2 are very similar. The main peak around 285 eV is mainly due to surface contamination (see Fig. 1 and compare C1s spectrum of the surface contamination in Fig. 2). The peak around 282.5 eV is assigned to C atoms being surrounded by boron. With further increasing N content, the C1s spectrum shows a sudden change. The peak around 282.5 eV moves to higher binding energies indicating that carbon has also bonds to a more electronegative partner than B, i.e. C or more likely N atoms. In the spectrum of the film deposited with 50% N_2, the contribution of binding energies <284 eV is very low meaning that only very few C atoms are bonded to B. The contribution of binding energies >285 eV indicates the presence of bonds between C and N. Nevertheless, this last assumption has to be treated with care because this sample had a strong surface contamination. Finally, the N1s spectra confirm the interpretation of both the B1s and C1s spectra. The dashed spectrum of the sample deposited without N_2 in the gas in Fig. 4 gives an impression of the contribution of the (small) surface contamination (approx. 3 at.% N at the surface, 0.5 at.% in the bulk). The spectrum of the film deposited with 2% N_2 in the gas has its maximum at 397.5 eV, whereas the shoulder towards higher binding energies could be due to the surface contamination. The observed N1s energy is lower as in h-BN (398.4 eV [31]) because the N atoms are completely embedded into less electronegative B atoms (average number of nearest neighbours >3 [8]) as already reported by Oliveira and Conde [53]. This is similar for the sample deposited with 4% N_2. Then, again for the deposition with 8% N_2 in the gas, the shape of the spectrum changes. The maximum moves to a binding energy corresponding to that of h-BN and the peak gets broader. Also, a small contribution at higher binding energies is observed that indicates bonds between N and C. The spectrum of the film deposited with 50% N_2 in the gas consists of at least two peaks where B–N bonds (lower energy) and C–N bonds (higher energy) can be supposed. However, the surface of this sample was strongly contaminated with carbon, and therefore, no conclusions can be drawn from the intensity ratio of the peaks.

Summarising, we found a change in the bonding characteristics with increasing N content in the amorphous films with B/C=4:1. Without N, we find B–B and B–C bonds and C is surrounded by B. For a small N content, B–N bonds are mainly formed and the N atoms are surrounded by B as well. If the N content is further increased (sample deposited with 8% N_2 in the gas, 34 at.% N in the film), there is not enough B to surround both C and N completely, therefore, bonds between C and N appear. In such a material, a real ternary bonding exists (bonds between all elements) but a phase separation begins. An even further increasing N content leads to a complete separation into microscopic BN and CN_x phases where no B–B or B–C bonds can be detected. The phase separation is confirmed by a more and more graphitic structure evidenced by the decreasing number of nearest neighbours and the appearance of the 8 eV peak in the low-loss EELS spectra [8].

4.4. Films deposited from the BC4 target

Now, we want to have a look at C-rich films (B/C ≈ 1:4) with increasing N content (spectra in Fig. 5). The FTIR spectrum of the sample without N shows two absorptions as mentioned above. The absorption at 700 cm^{-1} is assigned to (polarised) C–C stretching bonds and the much stronger absorption at 1250 cm^{-1} to B–C and C–C stretching bonds. With the incorporation of N, the absorption at 700 cm^{-1} gets first stronger and then broader to higher wavenumbers because of the contribution of the B–N–B bending at 780 cm^{-1}. The maximum of the main absorption shifts from 1250 to 1400 cm^{-1} and the peak gets broader. It consists of contributions from the B–N stretching bond at 1400 cm^{-1} but also from (polarised) C–C bonds what can be seen from the asymmetry to lower wavenumbers. The role of C–N bonds remains unclear as mentioned above. At a certain N content, the N–H stretching bond at 3400 cm^{-1} and the C≡N bond at 2200 cm^{-1} are observed. Especially, the latter gets much stronger when increasing the amount of N_2 in the gas from 25% to 100% while the N content in the films does not change significantly (from approx. 30 at.% to approx. 33 at.%) and the shape of the main absorption structure around 1400 cm^{-1} does not change either. From that, it can be concluded that additional N is incorporated in the form of the nitrile group (–C≡N).

XPS spectra were recorded for three samples only. The B1s spectrum of the film without N shows a two peak structure as mentioned above (lower energy: boron with incorporated C atoms, higher energy: B atoms in a carbon environment). When N is added, the peak at 188.8 eV disappears indicative of the reduced contribution from a B–B/B–C bonding environment. The peak at 191 eV remains, indicating that B is surrounded by more electronegative atoms. However, unlike the case without N in the film where this peak can be unequivocally assigned to B surrounded by C, now it could be also B surrounded by N atoms. This is confirmed by the C1s spectra. Without N in the film,

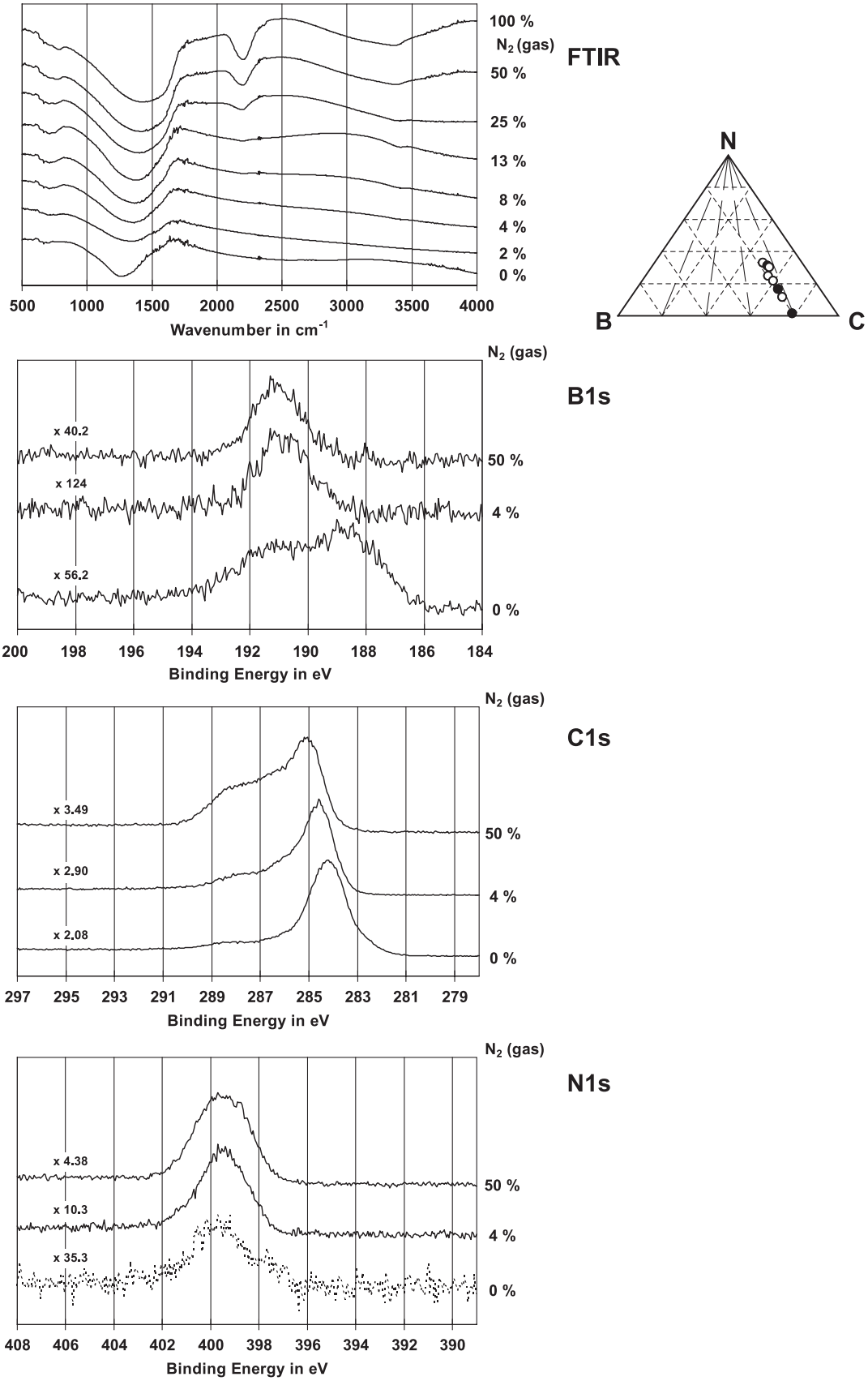

Fig. 5. Transmission FTIR, B1s, C1s and N1s XPS spectra (stacked) together with the bulk composition of samples deposited from the BC4 target. For the samples marked by empty circles in the composition graph, only FTIR measurements were done.

the maximum of the C1s is found at 284.2 eV suggesting a large amount of C–C bonds. The contribution at energies below 283 eV gives evidence of C bonded to B. This contribution disappears completely when N is incorporated. Since there are no more bonds between C and B then, the B atoms have to be bonded to N. On the other hand, the maximum of the C1s spectrum is shifted to higher binding energies with an increasing N content because C bonds to the more electronegative N. Here, the increasing variety of chemical surroundings of the C atoms is connected with the strong increase of the broad shoulder at higher energies. The N1s spectra do not show such a significant change. The dashed spectrum shows again the contribution of the surface contamination. In the spectra of films deposited with N_2 in the gas, two contributions are supposed. First, a single peak that corresponds to N atoms that surround the B atoms and separate them from the C atoms. Since these N atoms are bonded to B and C, their N1s energy is higher (approx. 399.5 eV) than in the case of h-BN (398.4 eV [31]). The second feature is the typical double peak structure of the spectrum observed for CN_x films with peaks at 398.5 and 400 eV. At low N content in the film (deposition with 4% N_2 in the gas), the first feature is dominant and the spectrum shows one sharp peak maximum rising over a broader ground structure. At higher N content (deposition with 50% N_2), the contribution of the double peak increases and so together with the single peak, a broad peak shape is formed where the double structure is not resolved.

The conclusions of the interpretation of all spectra from films with B/C ≈ 1:4 are the following. Without N in the film, B and C do not form a solid solution of the macroscopic composition but two separate microscopic phases. One phase is boron with a maximum number of incorporated C atoms. The other phase is carbon containing B as impurity atoms. When N is incorporated, it is first bonded to B separating B and C atoms. At this stage, a real ternary bonding is formed. With increasing N content, B–C bonds disappear until B is saturated with N. Then, any further N is bonded to C and a separation into microscopic BN and C/CN_x phases is observed.

5. Conclusions

The bonding characteristics of BCN films show a great variation range in dependence on their composition. Starting from pure boron, both C and N atoms are completely surrounded by boron. With increasing C- and/or N content, the number of nearest neighbours is decreasing [8]. In N-free films, there is a maximum number of C atoms that can be incorporated into boron. If more C atoms are added, two phases are formed. This is boron with the maximum C content (about 20 at.% according to our investigation) and a carbon phase containing B atoms as impurity. However, since without nitrogen, there is no volatile reaction product any macroscopic composition between pure boron and pure carbon can be adjusted. In contrast to that, the composition range of the N incorporation is limited to a maximum N content also on a macroscopic scale. There are mainly two volatile components formed in the film during the deposition process which limit the maximum N-incorporation. These are N_2 and C_2N_2. The latter is more important for the deposition with C-rich targets and may lead to an increase of the B/C ratio in the film compared to that in the target. Incorporating N into the film, first the B atoms are saturated by forming B–N bonds. During this process, B–C bonds disappear. At a certain N content, also C–N bonds are formed. Since more N can be bonded to B in comparison to C, the maximum N content depends on the B/C ratio in the film. However, at maximum N content, we find both BN and C/CN_x phases—the latter with a maximum of C≡N bonds for a given B/C ratio—and not an unique ternary bonded material. To conclude, in our amorphous films, real ternary compounds are only formed when at least one element is incorporated only in a small concentration and could be considered as impurity. Otherwise, a separation into binary and single phases is observed. Considering this, it will be very difficult or even impossible to deposit a real ternary material with any desired composition. Especially reports on real ternary materials with the composition BC_2N (cubic or graphitic structure) cannot be proved for amorphous films.

The great variety of bonding characteristics is connected with other structural properties such as number and distance of nearest neighbours, but also with the mechanical properties hardness and Young's modulus [8] which decrease in connection with the phase separation and have their minimum value at maximum N content. The maximum N content is probably a consequence of the disturbed resonance between electronic and atomic structure so that more N leads to an unstable structure [8].

To summarise, thin amorphous films of boron, carbon and nitrogen were deposited by reactive magnetron sputtering using targets of different B/C ratios and variable Ar/N_2 atmospheres. The bonding characteristics were obtained by a combined analysis of FTIR and XPS spectroscopies. We found a maximum solubility of carbon in boron of around 20 at.% in clear agreement with the crystalline BC phases. In the case of BCN compounds, real ternary phases, presenting B–C–N bonds, were only found at low nitrogen contents; in boron-rich films. At higher nitrogen contents, the FTIR and XPS spectra were dominated by BN, CC/CN and C≡N bonds, suggesting a phase separation into BN and C/CN_x phases.

References

[1] Z.F. Zhou, I. Bello, M.K. Lei, K.Y. Li, C.S. Lee, S.T. Lee, Surf. Coat. Technol. 128–129 (2000) 334.
[2] Y. Wada, Y.K. Yap, M. Yoshimura, Y. Mori, T. Sasaki, Diam. Relat. Mater. 9 (2000) 620.
[3] D. Hegemann, R. Riedel, C. Oehr, Thin Solid Films 339 (1999) 154.
[4] T. Komatsu, M. Samedima, T. Awano, Y. Kakadate, S. Fujiwara, J. Mater. Process. Technol. 85 (1999) 69.

[5] S. Nakano, M. Akaishi, T. Sasaki, S. Yamaoka, Chem. Mater. 6 (1994) 2246.
[6] S. Ulrich, H. Ehrhardt, T. Theel, J. Schwan, S. Westermeyr, M. Scheib, P. Becker, H. Oechsner, G. Dollinger, A. Bergmaier, Diam. Relat. Mater. 7 (1998) 839.
[7] V. Linss, I. Hermann, N. Schwarzer, U. Kreissig, F. Richter, Surf. Coat. Technol. 163–164 (2003) 220.
[8] V. Linss, J. Barzola-Quiquia, P. Häussler, F. Richter, Thin Solid Films doi:10.1016/j.tsf.2004.03.008.
[9] C. Ronning, H. Feldermann, R. Merk, H. Hofsäss, P. Reinke, J.-U. Thiele, Phys. Rev., B 58 (1998) 2207.
[10] F. Le Normand, J. Hommet, T. Szörényi, C. Fuchs, E. Fogarassy, Phys. Rev., B 64 (2001) 235416.
[11] M.O. Watanabe, S. Itoh, K. Mizushima, Appl. Phys. Lett. 68 (1996) 2962.
[12] F. Saugnac, F. Teyssandier, A. Marchand, J. Am. Ceram. Soc. 75 (1992) 161.
[13] J.H. Kaufmann, S. Metin, D.D. Saperstein, Phys. Rev., B 39 (1989) 13053.
[14] N.M. Victoria, P. Hammer, M.C. dos Santos, F. Alvarez, Phys. Rev., B 61 (2000) 1083.
[15] N. Nakayama, Y. Tsuchiya, S. Tamada, K. Kosuge, Jpn. J. Appl. Phys. 32 (1993) L1465.
[16] N. Vast, J.M. Besson, S. Baroni, A. Dal Corso, Comput. Mater. Sci. 17 (2000) 127.
[17] E. Pascual, M. Martínez, J. Esteve, A. Lousa, Diam. Relat. Mater. 8 (1999) 402.
[18] S. Ulrich, T. Theel, J. Schwan, H. Ehrhardt, Surf. Coat. Technol. 97 (1–3) (1997) 45.
[19] J. Yue, W. Cheng, X. Zhang, D. He, G. Chen, Thin Solid Films 375 (2000) 247.
[20] M.L. Kosinova, N.I. Fainer, Y.M. Rumyantsev, A.N. Golubenko, F.A. Kuznetsov, J. Phys., IV France 9 (1999) 915.
[21] Y. Wada, Y.K. Yap, M. Yoshimura, Y. Mori, T. Sasaki, Diam. Relat. Mater. 9 (2000) 620.
[22] J. Hu, P. Yang, C.M. Lieber, Phys. Rev., B 57 (1998) R3185.
[23] S.E. Rodil, A.C. Ferrari, J. Robertson, S. Muhl, Thin Solid Films 420–421 (2002) 122.
[24] B. Yao, L. Liu, W.H. Su, J. Appl. Phys. 86 (1999) 2464.
[25] H.S. Kim, I.H. Choi, Y.-J. Baik, Surf. Coat. Technol. 133–134 (2000) 473.
[26] S. Ulrich, A. Kratzsch, H. Leiste, M. Stüber, P. Schloßmacher, H. Holleck, J. Binder, D. Schild, S. Westermeyer, P. Becker, H. Oechsner, Surf. Coat. Technol. 116–119 (1999) 742.
[27] Z.F. Zhou, I. Bello, M.K. Lei, K.Y. Li, C.S. Lee, S.T. Lee, Surf. Coat. Technol. 128–129 (2000) 334.
[28] H. Künzli, PhD Thesis, University Basel, Switzerland, 1994 (in German).
[29] T. Hasegawa, K. Yamamoto, Y. Kakudate, Diam. Relat. Mater. 11 (2002) 1290.
[30] Z.M. Ren, Y.F. Lu, H.Q. Ni, Z.F. He, D.S.H. Chan, T.S. Low, K.R. Gamani, G. Chen, K. Li, Laser Processing of Materials and Industrial Applications II, Beijing, China, 1998, Proceedings of the SPIE—The International Society for Optical Engineering, vol. 3550, 1998, p. 93. (ISSN: 0277-786X).
[31] P. Reinke, P. Oelhafen, H. Feldermann, C. Ronning, H. Hofsäss, J. Appl. Phys. 88 (10) (2000) 5597.
[32] H. Werheit, M. Laux, U. Kuhlmann, R. Telle, Phys. Status Solidi, B Basic Res. 172 (1991) K81.
[33] S.E. Rodil, Recent Res. Dev. Appl. Phys. 6 (2003) 391.
[34] E. György, V. Nelea, I.N. Mihailescu, A. Perrone, H. Pelletier, A. Cornet, S. Ganatsios, J. Werckmann, Thin Solid Films 388 (2001) 93.
[35] T. Thärigen, G. Lippold, V. Riede, M. Lorenz, K.J. Koivusaari, D. Lorenz, S. Mosch, P. Grau, R. Hesse, P. Streubel, R. Szargan, Thin Solid Films 348 (1999) 103.
[36] L. Valentini, J.M. Kenny, G. Carlotti, M. Guerrieri, G. Signorelli, L. Lozzi, S. Santucci, Thin Solid Films 389 (2001) 315.
[37] Y.-B. Jiang, H.-X. Zhang, D.-J. Cheng, S.-Z. Yang, Thin Solid Films 360 (2000) 52.
[38] J.M. Ripalda, I. Montero, L. Galán, Diam. Relat. Mater. 7 (1998) 402.
[39] A. Laskarakis, S. Logothetidis, C. Charitidis, M. Gioti, Y. Panayiotatos, M. Handrea, W. Kautek, Diam. Relat. Mater. 10 (2001) 1179.
[40] M.E. Ramsey, E. Poindexter, J.S. Pelt, J. Marin, S.M. Durbin, Thin Solid Films 360 (2000) 82.
[41] L. Maya, L.A. Harris, J. Am. Ceram. Soc. 73 (1990) 1912.
[42] W.T. Zheng, E. Broitman, N. Hellgren, K.Z. Xing, I. Ivanov, H. Sjöström, L. Hultman, J.-E. Sundgren, Thin Solid Films 308–309 (1997) 223.
[43] Y. Etou, T. Tai, T. Sugiyama, T. Sugino, Diam. Relat. Mater. 11 (2002) 985.
[44] D. Marton, K.J. Boyd, A.H. Al-Bayati, S.S. Todorov, J.W. Rabalais, Phys. Rev. Lett. 73 (1994) 118.
[45] W.T. Zheng, J.H. Guo, Y. Sakamoto, M. Takaya, X.T. Li, P.J. Chao, Z.S. Jin, K.Z. Xing, J.-E. Sundgren, Diam. Relat. Mater. 10 (2001) 1897.
[46] D. Marton, K.J. Boyd, J.W. Rabalais, Int. J. Mod. Phys. B 9 (1995) 3527.
[47] F. Rossi, B. André, A. van Veen, P.E. Mijnarends, H. Schut, F. Labohm, M.P. Delplancke, K. Hubbard, J. Mater. Res. 9 (1994) 2440.
[48] L. Galán, I. Montero, F. Rueda, Surf. Coat. Technol. 83 (1996) 103.
[49] J.M. Ripalda, F.J. García de Abajo, I. Montero, L. Galán, M.A. Van Hove, Appl. Phys. Lett. 77 (2000) 3394.
[50] J.M. Ripalda, N. Díaz, I. Montero, F. Rueda, L. Galán, J. Appl. Phys. 92 (2002) 644.
[51] J.M. Ripalda, E. Román, L. Galán, I. Montero, S. Lizzit, A. Baraldi, A. Comelli, G. Paolucci, A. Goldoni, J. Chem. Phys. 118 (2003) 3748.
[52] K. Yamamoto, M. Keunecke, K. Bewilogua, Zs. Czigany, L. Hultman, Surf. Coat. Technol. 142–144 (2001) 881.
[53] M.N. Oliveira, O. Conde, J. Mater. Res. 16 (2001) 734.